High Speed VCSELs With Separated Quantum Wells

V. V. Lysak[1,2], I. M. Safonov[2],
Y. M. Song[1], I. A. Sukhoivanov[1,3],
Yong Tak Lee[1]

[1]*Department of Information and Communications, Gwangju Institute of Science and Technology*
1, Oryong-dong, Buk-ku, Gwangju, 500-712, Republic of Korea
[2] *Kharkov National University of Radio Electronics 14, Lenin ave., 61166, Kharkov, Ukraine*
[3]*Departamento de Electronica, FIMEE, Universidad de Guanajuato, Mexico*
Email: lysak@gist.ac.kr)

NUSOD 2008 September 1 - 4, 2008 /University of Nottingham, UK

Computers: past, present and future

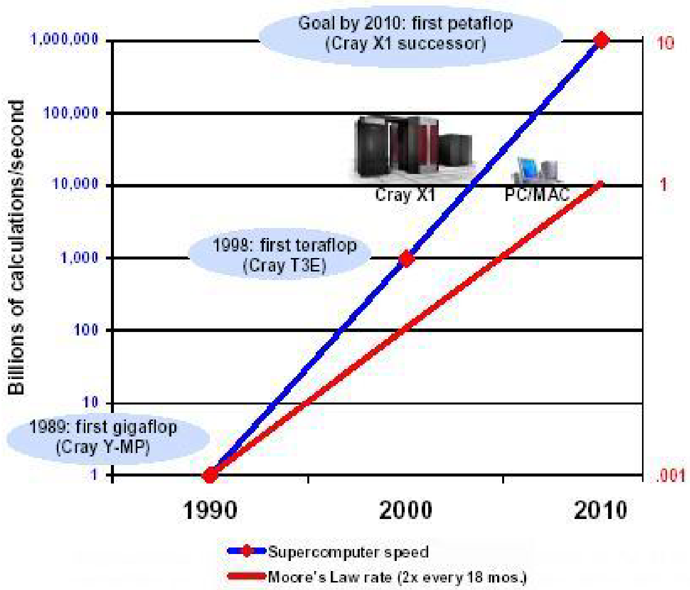

Cray1 1980s

Pocket PC 2000s

Cray X1 2000s

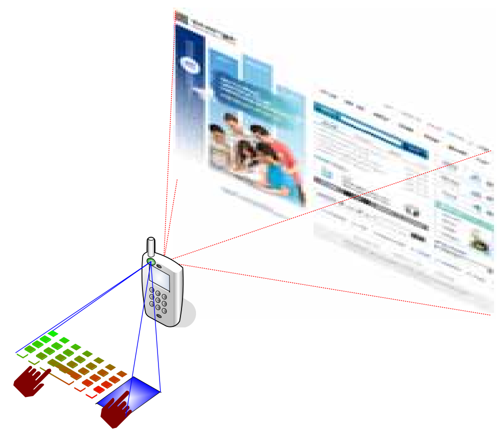

PC 2020s

Computer I/O architecture history and I/O roadmap

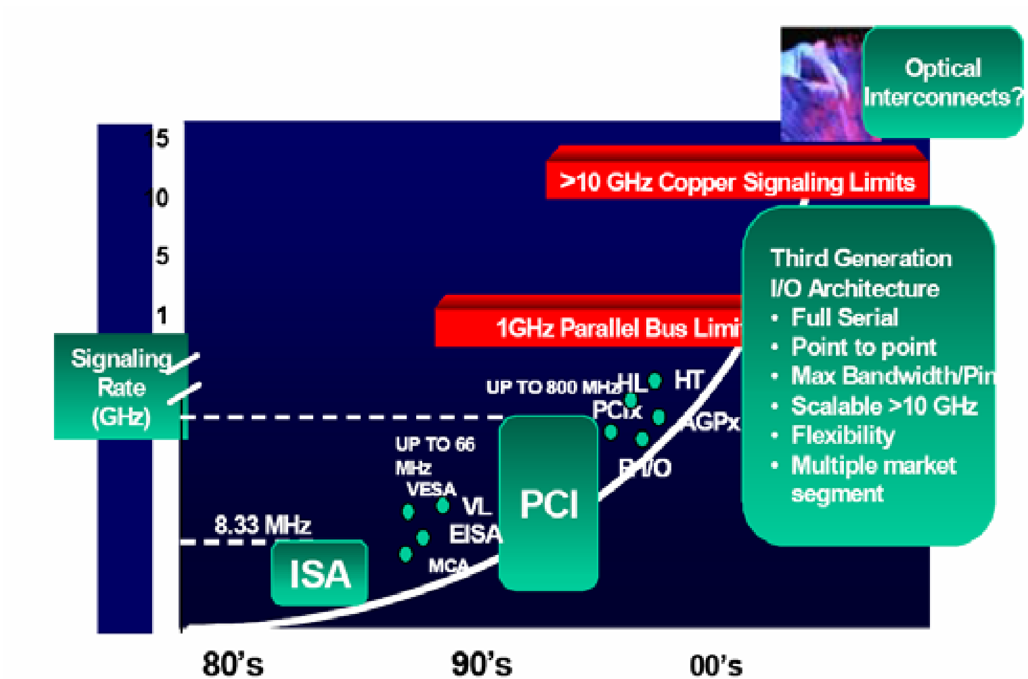

Beyond 10 GHz, copper interconnects, become bandwidth limited due to frequency-dependent losses such as **the skin effect in the conductors** and **the dielectric loss from the substrate material.**

We need the optoelectronic devices with

- good performance (high-modulation bandwidth, low power consumption, high efficiency)
- manufacturing advantages (amenable to high-volume production, wafer-level testing, and ease of integration).

E. Mohammed et.al, Intel Technology Journal, V.8 N.2, 2004, pp. 115-127

Demonstrator for chip-to-chip optical interconnects on the optical PCB

- Optical-fiber embedded PCB

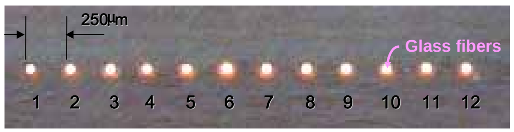

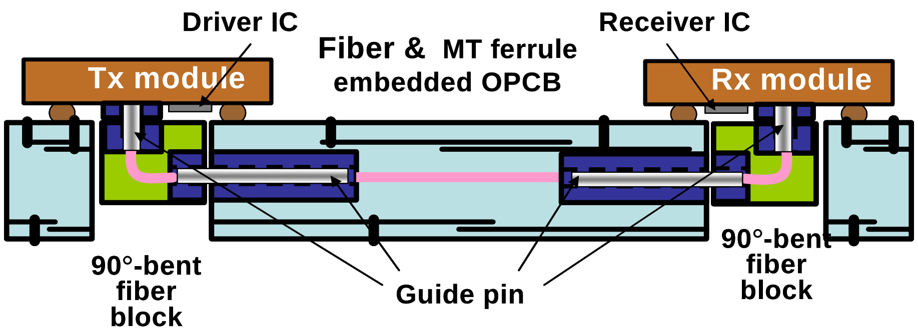

- VCSEL array

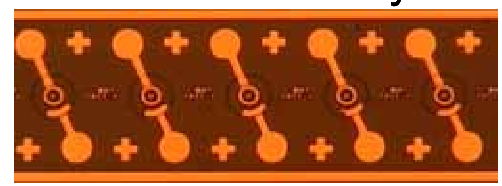

- Transmission test result

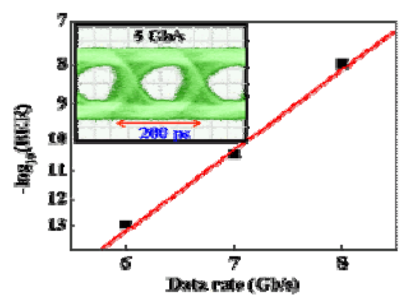

- 90° bent optical connector

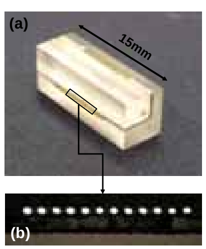

- Optical interconnection platform

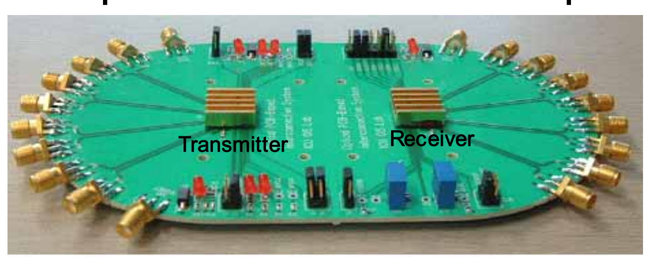

M. H. Cho, et. al, *IEEE PHONIC. TECH. L.*, 17, 690 (2005).

Intracavity contacted VCSEL array

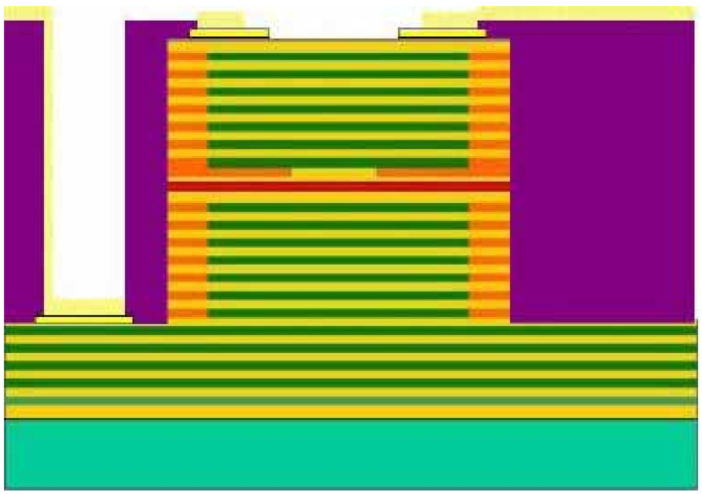

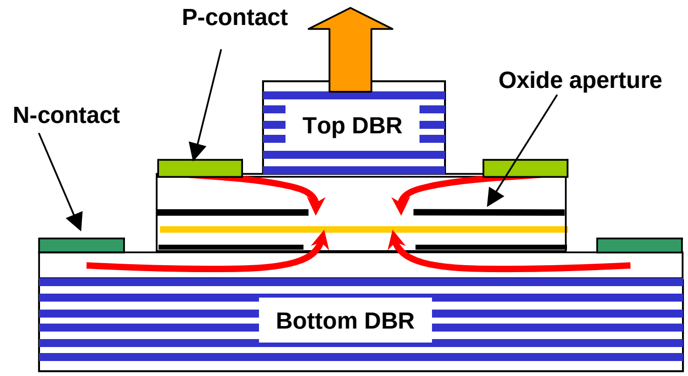

+ *Bypass the current flow through mirrors*
  ⇒ *lowers the series resistance*
+ *Use of undoped DBR mirror*
  ⇒ *reduce free carrier absorption*
  ⇒ *better reflectivity*
+ *Co-planar contact*
  ⇒ *suitable for flip-chip bonding*

Experimental part

L-I-V characteristics

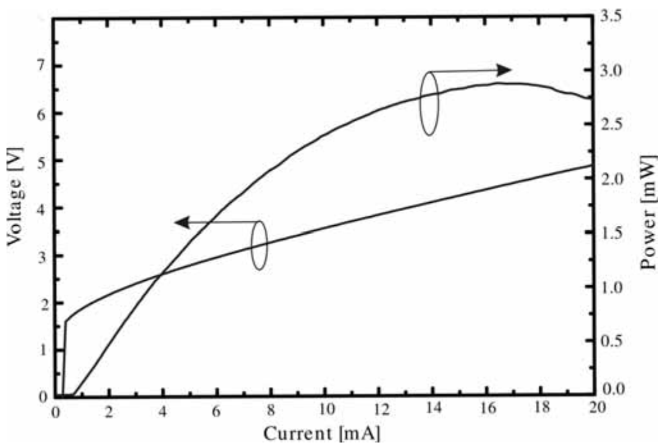

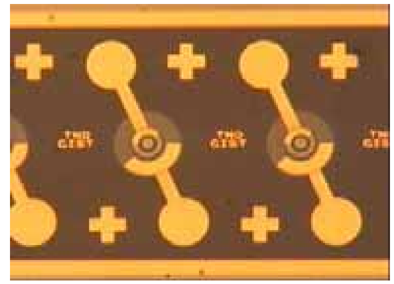

♦ small signal modulation

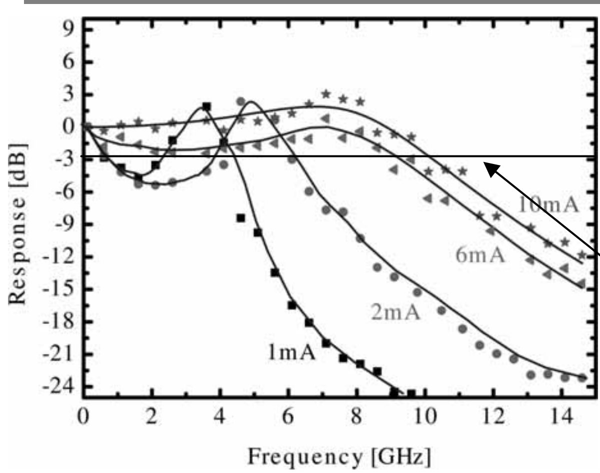

- **Oxide aperture dia. : 5 μm**
- **Threshold current : 0.7±0.05 mA**
- **Threshold voltage : 1.7 V**
- **Slope efficiency : 0.36±0.01 W/A @ I=2mA**
- **Differential quantum efficiency:**

  28.4±0.7 %@ I=2mA
- **Differential resistance : 150 Ω @ I=6mA**

3dB bandwidth 10 GHz at 10 mA

Axial enhancement factor

Resonance frequency

$$f_R = \frac{1}{2\pi}\sqrt{\eta_i \frac{\Gamma \xi v_g}{qV_{eff}} \frac{\partial g}{\partial N}(I - I_{th})}$$

$$V_{eff} = \pi R^2 (L_{pen,top} + L_{cav} + L_{pen,bot})$$

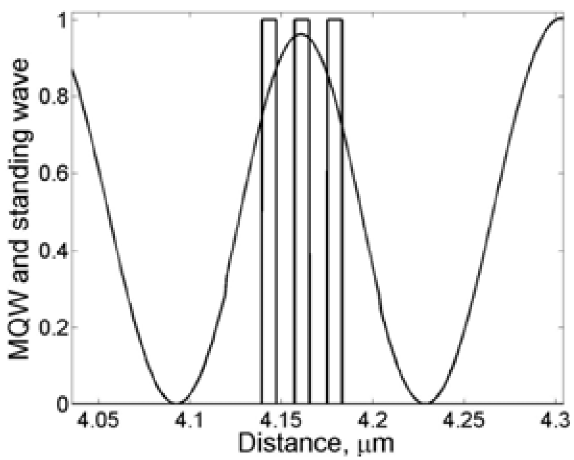

1.79

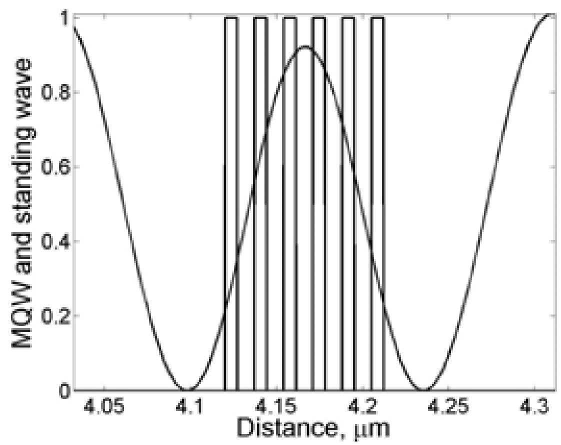

1.2

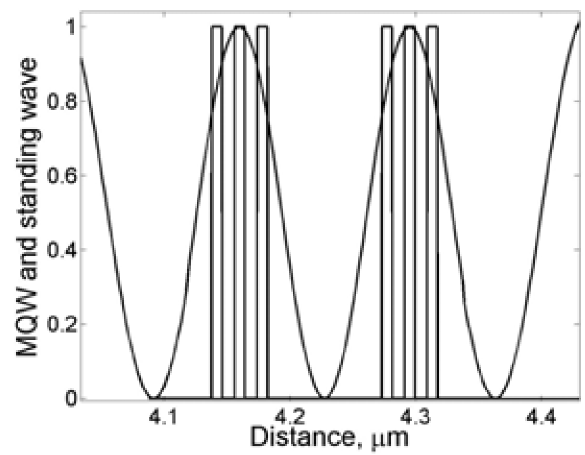

1.85

Interactions between physical processes in LD

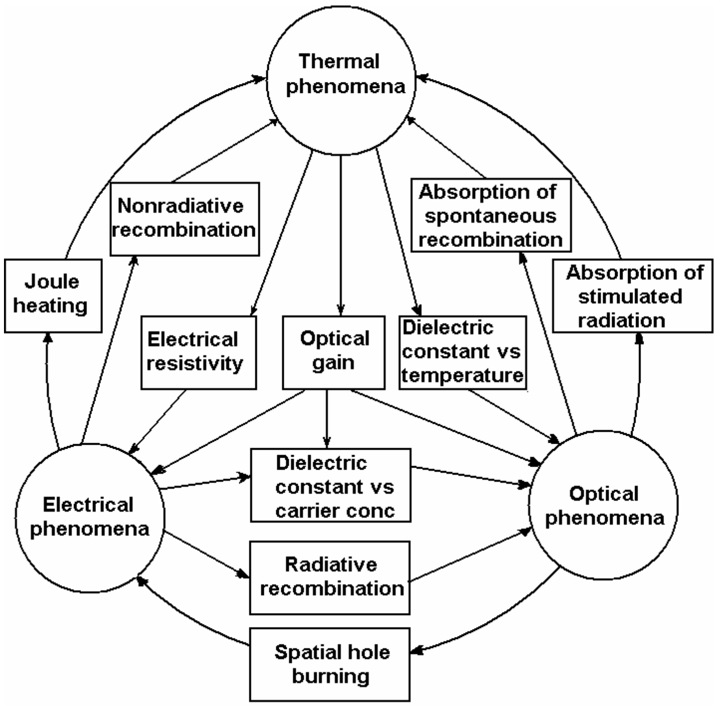

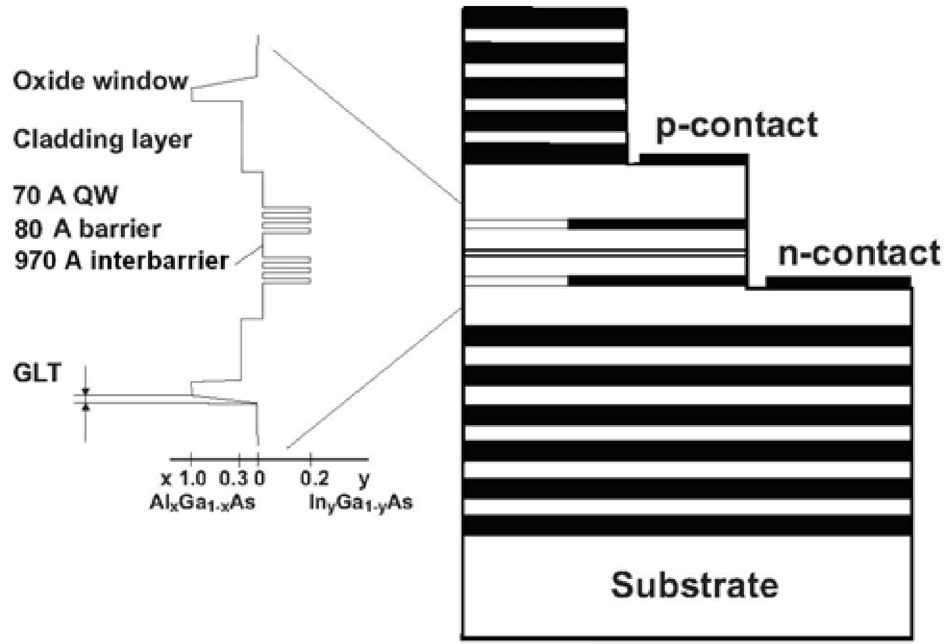

Vertical-cavity surface-emitting laser devices/ ed. by H.E.Li, K.Iga. (Springer series in photonics; v.6), Ch. 5

Optical field solution

For homogeneous lossless medium Maxwell's equations can be transformed to vector wave equations

$$\left(\nabla^2 + k_0 n_R^2 \Psi\right) = 0$$

$$k_0 = \omega / c$$

Wave vector

$$n_{RA} = \begin{cases} n_{R1} & |r| \le r_A \\ n_{R2} & |r| \ge r_A \end{cases}$$

for index-guiding structure

Common solution of electric field distribution in active layer

$$E_T^{k,m,s} = E_{k,m,s} \exp(ik\phi) \exp(i\beta_z z) \begin{cases} J_k\left(\dfrac{ur}{r_A}\right) / J_k(u) & |r| \le r_A \\ K_k\left(\dfrac{vr}{r_A}\right) / K_k(v) & |r| \ge r_A \end{cases}$$

The standing optical wave of the fundamental mode

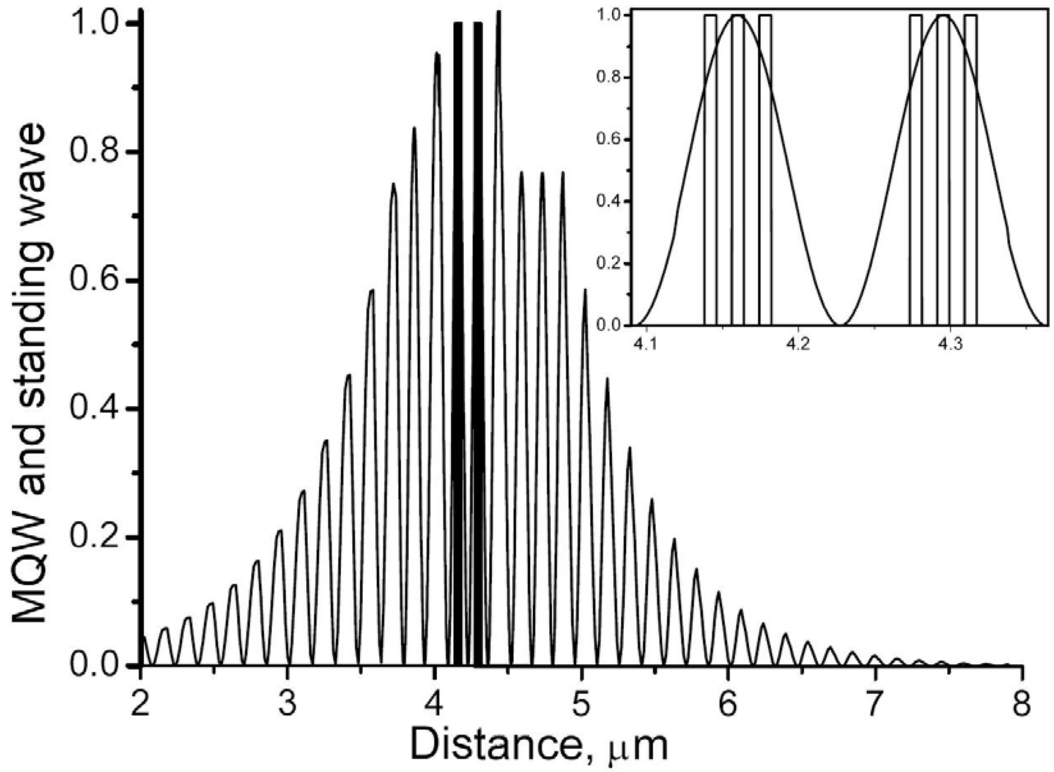

- The 980 nm VCSEL active layer contains a pair of three 70/80Å $In_{0.2}Ga_{0.8}As/GaAs$ QWs/barriers, separated by the inter-barrier designed to place a QWs in a maxima of generated field

Electrical phenomena

Poisson equations

$$\nabla \cdot \varepsilon \nabla V = -e\left(p - n + N_D^+ - N_A^-\right)$$

Current density of electrons and holes

$$j_n = -e\mu_n \nabla V + eD_n \nabla n + eD_n^T \nabla T$$
$$j_p = -e\mu_p \nabla V - eD_p \nabla p - eD_p^T \nabla T$$

mobility diffusion thermal diffusion

Continuity equations for electrons and holes

$$\frac{\partial n}{\partial t} = \frac{1}{e}\nabla \cdot j_n + (G - R),$$
$$\frac{\partial p}{\partial t} = -\frac{1}{e}\nabla \cdot j_p + (G - R).$$

Carrier generation rate

$$G = \frac{|j_n|}{eL_z} = \frac{|j_p|}{eL_z}$$

Carrier recombination rate

$$R = \underbrace{R_{sp} + R_{st}}_{radiative} + \underbrace{R_{SRH} + R_A}_{nonradiative}$$

Energy band distribution

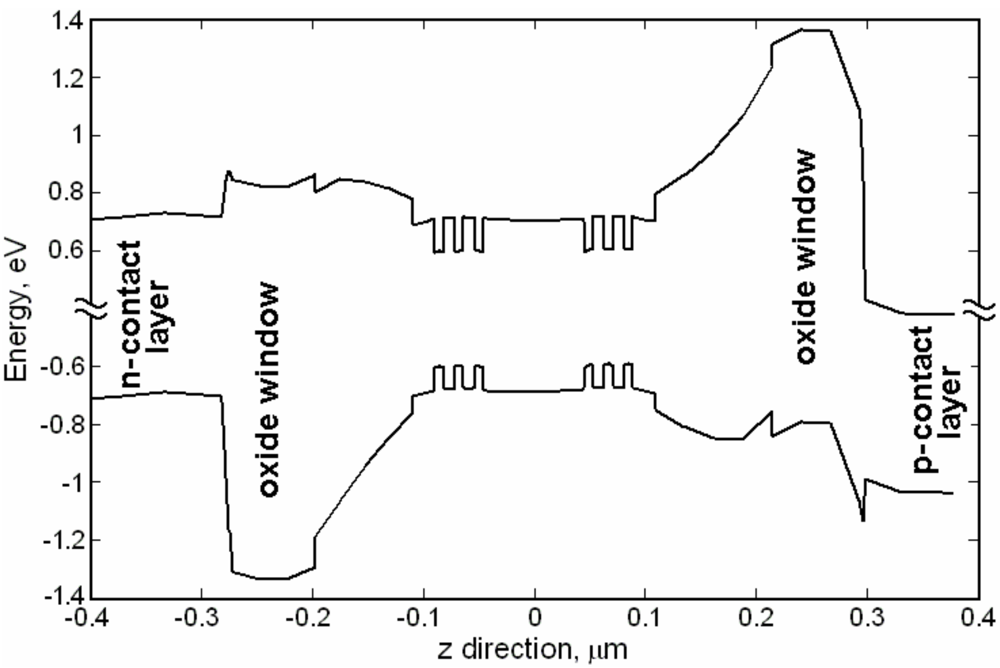

Electron current magnitude for different pumping currents

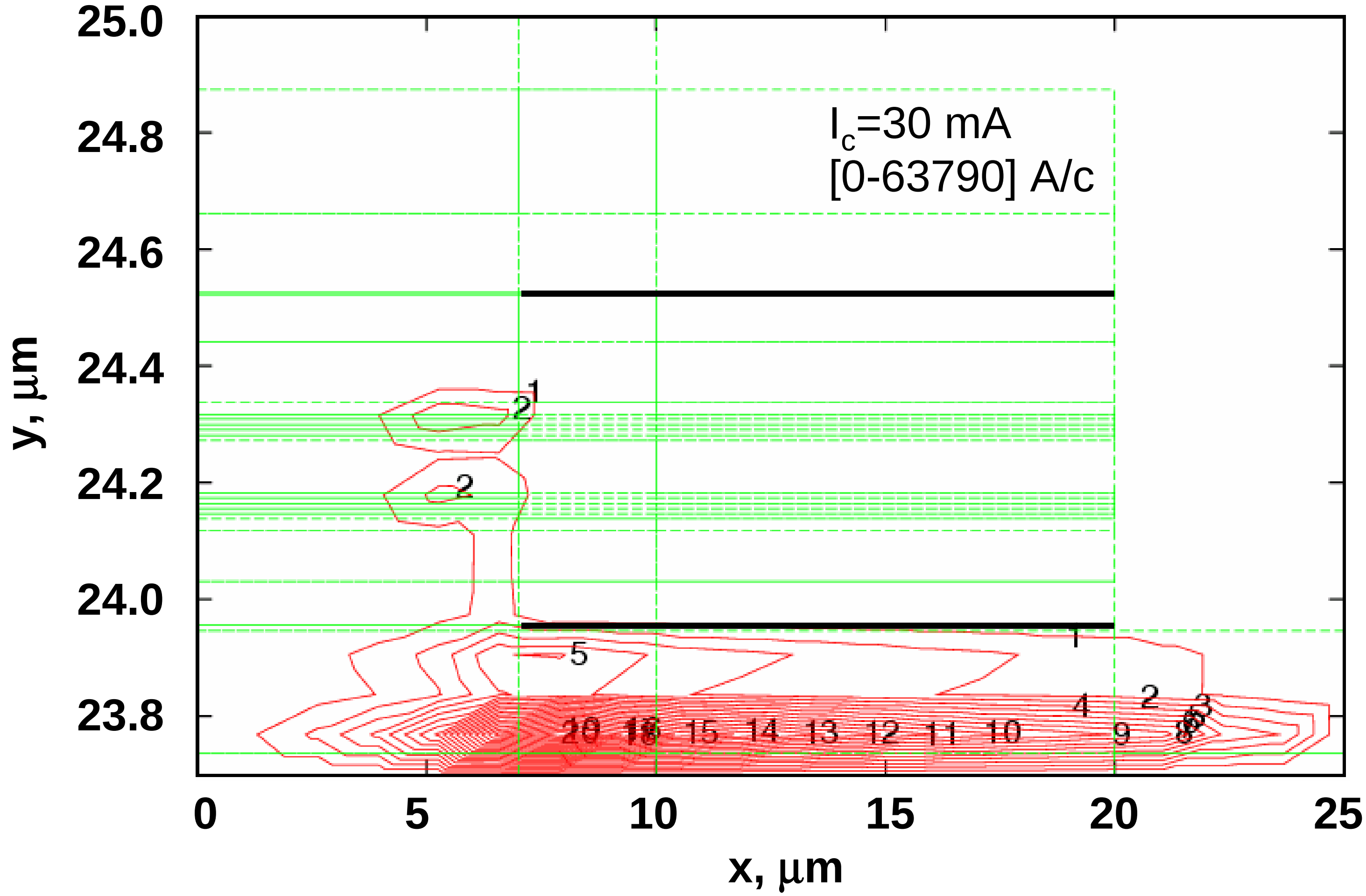

Thermal phenomena

Basic thermal equation

$$C_P \rho \frac{\partial T}{\partial t} = \nabla \cdot \kappa \nabla T + H$$

- C_P: Heat coefficient
- ρ: Material density
- κ: Thermal conductivity
- H: Heat sources

$$H = H_{Joule-dc} + H_{Joule-op} + H_{rec} + H_T + H_P$$

$H_{Joule-dc}$	~17 %	Steady-state Electrical field
$H_{Joule-op}$	~ 1 %	Optical wave absorption on loss semiconductors
H_{rec}	80 %	Recombination heat
H_T	0.001 %	Thomson heat
H_P	~ 2 %	Peltier heat

Power versus current

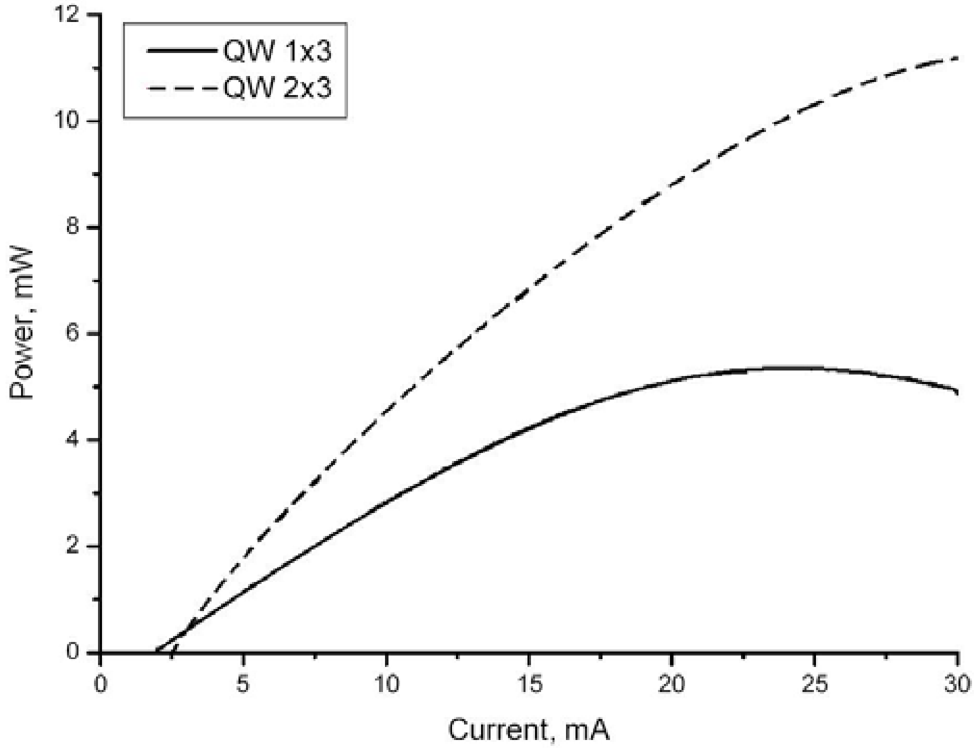

The modulation conversion efficiency factor

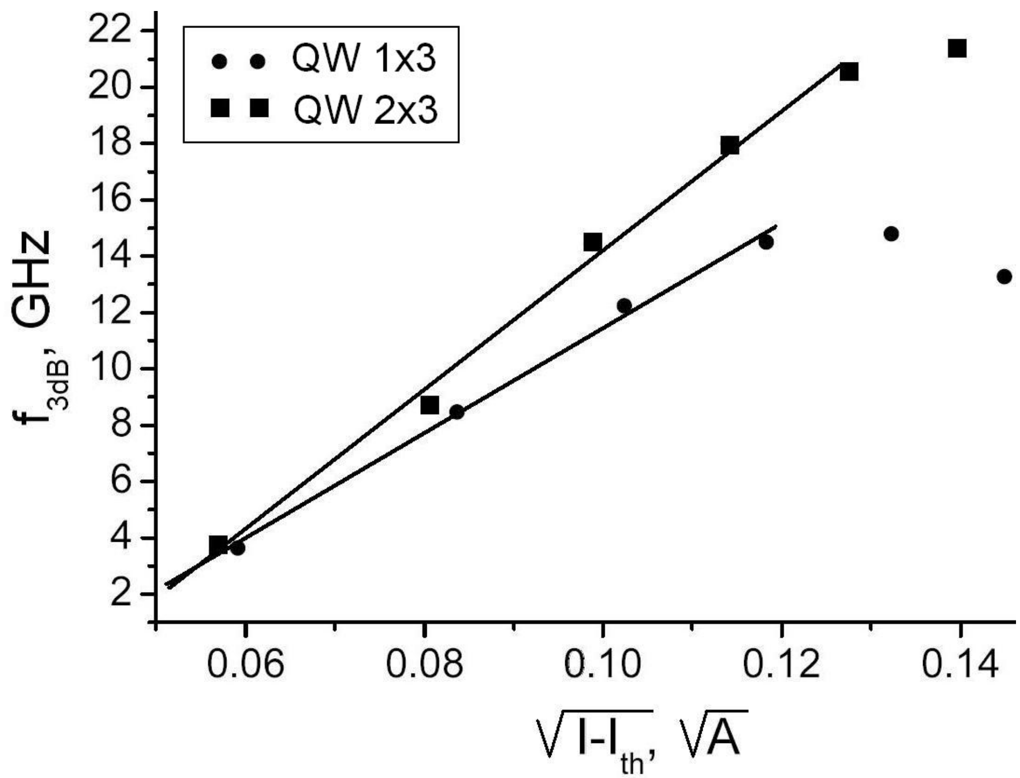

The solid lines present the fitting with modulation conversion efficiency factor of 159 and 240 GHz/(A)$^{0.5}$ for device with one and two triplets of QWs, respectively

Conclusion

- we have analyzed the thermal, electrical, optical, and modulation properties of the 980 nm InGaAs ICOC VCSELs with different structures of active layer
- Results show inserting quantum wells in maxima of the generated field increases the slope efficiency of L-I characteristic due to increasing the modal gain of device
- The analysis of modulation characteristics clarify that devices with two triplets of QWs have wider modulation bandwidth and the modulation conversion efficiency factor is approximately 240 GHz/(A)$^{0.5}$ due to more efficient position of QWs in the resonator.

This work is supported by MOE through the
BK21 Program and by MOST through TND Project of Korea